산업기술연구(강원대학교 산업기술연구소 논문집) 제17집, 1997
Research Report. The Institute of Industrial Technology, Kangwon Nat'l Univ., Korea, Vol.17, 1997

천음속유동에서 초임계익형의 후연확대수정의 영향

유 능 수*

Effect of Divergent Trailing Edge Modification of Supercritical Airfoil in Transonic Flow

Yoo, Neung-Soo*

ABSTRACT

The computation of the flow around a supercritical airfoil with a divergent trailing edge(DTE) modification(DLBA 243) is compared to that of original supercritical airfoil(DLBA 186). For this computation, Reynolds-Averaged Navier-Stokes equations are solved with a linearized block implicit ADI method and a mixing length turbulence model. Results show the effects of the shock and separated flow regions on drag reduction due to DTE modification. Results also show that DTE modification accelerates the boundary layer flow near the trailing edges which has an effect similar to a chordwise extension that increases circulation and is consistent with the calculated increase in the recirculation region in the wake. Airfoil with DTE modification achieves the same lift coefficient at a lower incidence and thus at a lower drag coefficient, so that lift-to-drag ratio is increased in transonic cruise conditions compared to the original airfoil. The reduction in drag due to DTE modification is associated with weakening of shock strength and delay of shock which is greater than the increase in base drag.

1. INTRODUCTION

Supercritical airfoils first developed by Whitcomb[1] were designed to decrease the strength of shock and move it rearward. Supercritical airfoils have a rooftop pressure distribution[1] which implies nearly parallel upper and lower surfaces near the trailing edge.[2] If the trailing edge is sharp, then the geometry is thin in this highly loaded aft region, so blunt trailing edges are often preferred in practice despite of the additional drag of the blunt base.[3]

Henne and Gregg designed divergent trailing edge(DTE) airfoils to reduce drag creep on blunt supercritical airfoils at high subsonic Mach numbers.[4] They started with an existing supercritical airfoil(DLBA 186) as the original geometry, and created a new DTE airfoil(DLBA 243) by increasing the airfoil thickness over the aft 10% of chord such that suction and pressure side flow diverge from each other at the trailing edge as shown in Fig.1. This DTE modification to a blunt supercritical airfoil increases the size of the recirculation zone in the wake[5], so increases the lift-to-drag ratio and improves airfoil performance.

Transonic aerodynamics of DTE airfoils were calculated[6] by solving Euler equation and integral boundary layer equation using the viscous-inviscid interaction procedure of Bauer, Garabedian and Korn.[2] The use of boundary layer equation forces two approximations: the

* 강원대학교 정밀기계공학과 교수

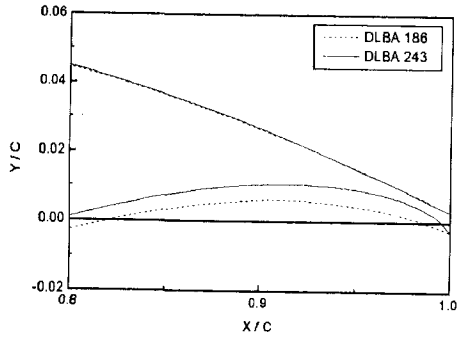

first, the shape of the recirculation in the wake must be specified empirically by locating the streamline that divides forward and reverse flow in the wake of the divergent trailing edge; and the second, an experimental correlation must be used to estimate base drag since the code cannot calculate any variables in this region, which includes the surface pressure on the aft-facing base. Henne correlated calculated results with experiments at cruise conditions but, since the flow immediately aft of the trailing edge was guessed, the relationship between the recirculation region and lift-to-drag ratio remains uncertain.

Previous experiments and calculations of divergent trailing edge airfoils did not consider the nature of the recirculating flow in the wake, despite the well-established upstream influence of the merging suction side and pressure side wake flow on the surface pressure near the trailing edge.[7] Measurements in the small recirculation region downstream of the blunt divergent trailing edge are extremely difficult and expensive. Any measurements of this region have not been reported to date, probably because its cross stream and streamwise dimensions are about between 0.5% and 2% of chord.

The present approach uses a validated computational approach to improve the understanding of the relationship between the recirculating flow in wake and the drag reduction associated with DTE modification. Navier-Stokes equation is solved here to accurately represent trailing-edge recirculation regions and shock wave phenomena and to quantify the influence of the recirculation region on the suction side shock and aerodynamic performance. The following section describes the present Navier-Stokes computational procedure including solution algorithm, grid generation, boundary conditions and turbulence model. Numerical uncertainty and grid independence are quantified. Calculation of flow around the original supercritical airfoil(DLBA 186) and that of flow around the DTE airfoil(DLBA 243) are presented to quantify boundary layer development and shock strength. The paper ends with summary remarks about the flow and transonic shock around DTE airfoils and their influence on drag reduction.

2. COMPUTATIONAL METHOD

2.1 Solution Algorithm

The two-dimensional, Reynolds-Averaged, Navier-Stokes equation is solved here in conservative form with the linearized block implicit numerical procedure of Briley and McDonald[8] which employs centered spatial differences with adjustable numerical dissipation. The following equations for mass and momentum conservation are solved:

Continuity Equation

$$\frac{\partial \overline{\rho}}{\partial t} + \frac{\partial}{\partial x}(\overline{\rho u}) + \frac{\partial}{\partial y}(\overline{\rho v}) = 0$$

Momentum Equation

$$\frac{\partial}{\partial t}(\overline{\rho u}) + \nabla \cdot (\overline{\rho u V_\infty}) = -\frac{\partial \overline{p}}{\partial x} + \frac{\partial \overline{\tau_{xx}}}{\partial x} + \frac{\partial \overline{\tau_{yx}}}{\partial y} + \frac{\partial}{\partial x}(-\overline{\rho u' u'}) + \frac{\partial}{\partial y}(-\overline{\rho u' v'})$$

$$\frac{\partial}{\partial t}(\overline{\rho v}) + \nabla \cdot (\overline{\rho v V_\infty}) = -\frac{\partial \overline{p}}{\partial y} + \frac{\partial \overline{\tau_{xy}}}{\partial x} + \frac{\partial \overline{\tau_{yy}}}{\partial y} + \frac{\partial}{\partial x}(-\overline{\rho v' u'}) + \frac{\partial}{\partial y}(-\overline{\rho v' v'})$$

where

V_∞ ; free stream velocity , t ; time

u v w ; x, y, z velocity components

p ; pressure, τ_{ij} ; stress components
superscript bar ; average quantity
superscript ′ ; turbulent fluctuation

Shock capturing is used to determine the location of the shock. A region with increased grid density is placed in the anticipated shock location. This approach is advantageous when the exact shock locations are unknown.

For high Reynolds numbers, it becomes necessary in the present procedure to introduce an artificial viscosity or dissipation factor into the discretized transport equations. The artificial viscosity term is preceded by a constant, which is essentially the inverse of cell Reynolds number. The value of artificial viscosity is selected by the user to control the amount of artificial viscosity added in various regions of the flow field, and to allow its value to be reduced as the solution proceeds. In the present calculations it is initially set equal to 0.5 for the first 400 time steps then reduces to 0.05 following the recommendations of Briley and McDonald.[8]

The turbulence model used in this study is selected based on simplicity while providing reasonable accuracy. Mixing length turbulence model is chosen because it has been successfully used for transonic flow calculations. The mixing length turbulence model, although very simple, has provided good agreement when compared to experiments and calculations with the $\kappa-\varepsilon$ model, and the present calculations compare favorably with RAE 2822 experiments in previous work.[5][8][9]

2.2 Validation of Computations

The above CFD procedure needs to be validated by comparison with measurements. Transonic flow around an RAE 2822 airfoil exhibits boundary layer and shock characteristics similar to those on DTE airfoils. The 1980-1981 Stanford Conference[10] assessed an RAE 2822 experiment and by subsequent recommendations[11], so it is chosen to validation the CFD procedure described above.

The distribution and spacing of nodes, the outer computational boundaries, and the boundary conditions are implemented as described above. To be able to use the H-grid, a slight modification of the airfoil is necessary. The upper and lower surfaces are terminated at 99% of the chord where the trailing edge thickness is 0.0057 chord. This makes the airfoil shape more comparable to the blunt DTE airfoils.

This calculation is a good representation of the flow over the RAE 2822 airfoil.[5] Calculated value and measured value of the pressure coefficient on airfoil surfaces, are in excellent agreement as shown in Fig.2(COM = computational result, EXP = experimental result M = Mach number, AOA = angle of attack, RE = Reynolds number, CL = lift coefficient, CD = drag coefficient). Flow structures are resolved in the very small recirculation region downstream of the blunt trailing edge, and this should be more adequate resolution for the supercritical airfoils.

Calculations are judged to be converged when the change in lift coefficient per time step is less than 3×10^{-5}, and typically required about 1000 time steps. For selected calculations, iteration is continued to 1400 time steps.

Grid convergence is quantified by comparison of calculated results on coarse, medium and fine grids with 140 x 95, 185 x 125 and 235 x 160 nodes in streamwise and cross streamwise directions. Distributions of surface pressure show the maximum increment in local pressure

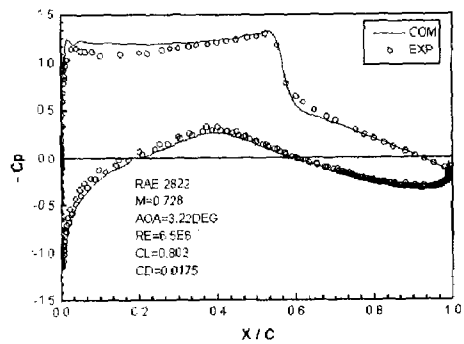

Fig.2 Calculated and Measured Pressure Coefficient of RAE 2822 Airfoil

decreases from 1.4% to 0.4% of the local pressure coefficient for these two grid refinement steps. The corresponding changes in lift and drag coefficients are about 2% and 8.5% between small and medium grids, and about 0.001% and 5.5% between medium and fine grids. The percentage error in drag is larger because drag is about an order of magnitude smaller than lift and is also more sensitive to numerical and modeling approximation.

Approximate quantification of numerical uncertainty in the present calculations[5] suggests calculated values within 0.3 and 6 percent of lift and drag, respectively. These estimates are obtained with the assumption that the solution for finer grids asymptotically approaches the correct solution, which is achieved in the limit of the spacing approaching zero. A grid convergence index(GCI) based on Richardson number interpolation is calculated for uniform grid refinement, and gives an conservative error estimate for a second order numerical method, such as that used here.[12] Results show asymptotic convergence in aerodynamics coefficients and, for the 185 by 125 grid, the calculated value of GCI for the lift coefficient is 0.03% which implies the 185 by 125 node grid is adequate and is used for the results presented below.

3. RESULTS

Computational results for velocity and pressure distributions are presented to provide insight into the flow structures that result in a reduction of drag creep with DTE modification. Calculations are presented here for the seed and DTE supercritical airfoils with trailing edge thicknesses of 0.57% of chord. Table 1 compares calculated and measured values of lift coefficient, drag coefficient, lift-to-drag ratio for both airfoils at the angle of attack and Mach number reported for the experiment. Comparisons between airfoils are made at a constant lift coefficient since lift and drag are the main design parameters, the angle of attack at which these values are achieved is of less importance. These coefficients are extremely sensitive to small changes in incidence and Mach number and when these values are varied within the reported experimental uncertainty, agreement is within 2% and 5% for lift and drag respectively.

Table 1 Calculated and Measured Aerodynamic Coefficients and Shock Location

airfoil	exp or com	AOA (deg)	M	C_L	C_D	L/D
DLBA186	exp	1.809	0.74	0.813	0.0122	66.6
	com		0.74	0.857	0.0138	62.1
DLBA243	exp	0.904	0.74	0.805	0.0101	79.7
	com	0.680	0.726	0.799	0.0105	76.1

Fig.3a shows an H-grid for the seed supercritical DLBA 186 airfoil with 185 x 125 nodes. Flow around this supercritical airfoil is calculated for the experimental conditions reported by Henne and Gregg[4] which were incidence(=AOA) of 1.809 degrees, transition fixed at 5% of chord where the boundary layer trip wire was located in the experiment. Maximum uncertainties in the measured values of incidence and Mach number were reported by Henne and Gregg[4] to be about 0.4 degrees and 0.02, respectively, which is consistent with other transonic wind tunnel measurements.

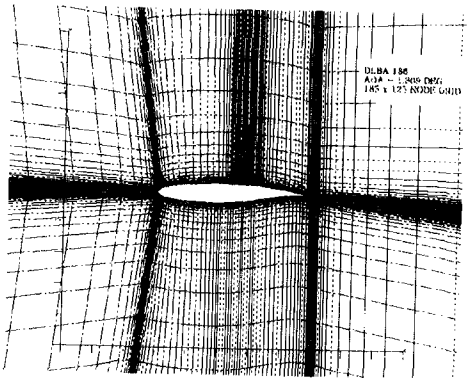

Fig.3a H-Grid for DLBA 186

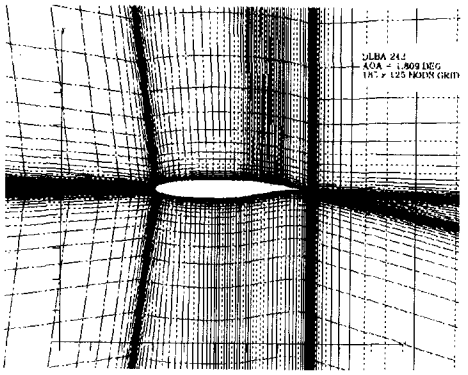

Fig.3b H-Grid for DLBA 243

Fig.3b shows the grid for the DTE DLBA 243 airfoil at 1.809 ° angle of attack(=AOA). This grid is almost identical to the supercritical seed grid with the exception of the concentration of nodes in the shock capture zone which is located appropriately further aft on the upper surface. Henne and Gregg[4] measured a lift coefficient(C_L) of 0.805 at 0.904 degree of AOA for the DTE airfoil. The best calculated match is shown on Table 1 for 0.68 degree incidence at a Mach number(=M) of 0.726, which is within experimental uncertainty.

Fig.4a and 4b show the pressure contours around DLBA 186 and DLBA 243 airfoils at a lift coefficient of 0.8, respectively. The DTE airfoil has a weaker, delayed shock compared to the seed airfoil. This is very well illustrated on Fig.5. Fig.6a and Fig.6b show the surface pressure distribution over these two airfoils at M=0.73 and M=0.76, and shows the reduction in shock strength and the delay of shock on the

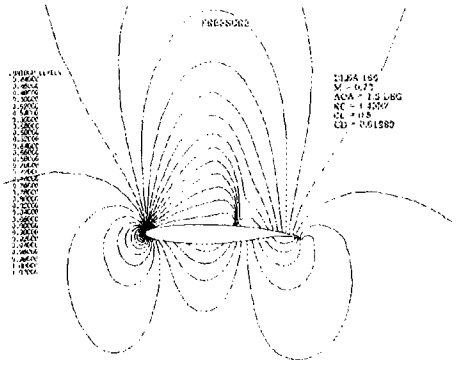

Fig.4a Pressure Contours around DLBA 186

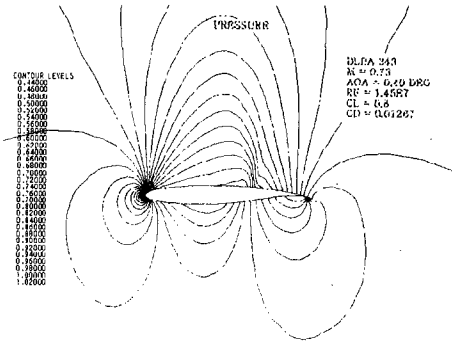

Fig.4b Pressure Contours around DLBA 243

M = 0.73 RE = 1.45E7 CL = 0.8

	DLBA 186	DLBA 243
AOA	1.2 DEG	0.49 DEG
CD	0.01283	0.01267

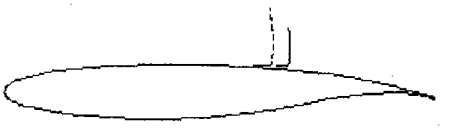

Fig.5 Shock Location and Strength

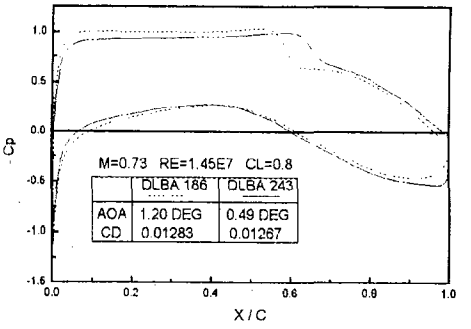

Fig.6a Surface Pressure Distribution - I

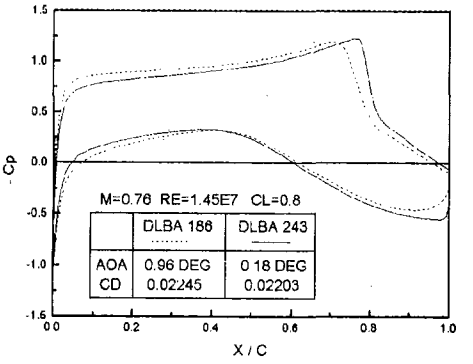

Fig.6b Surface Pressure Distribution - II

DTE airfoil. Fig.7a and 7b show velocity vectors in the trailing edge region. The recirculation region of DLBA 243 DTE airfoil is greater than that of DLBA 186 airfoil.

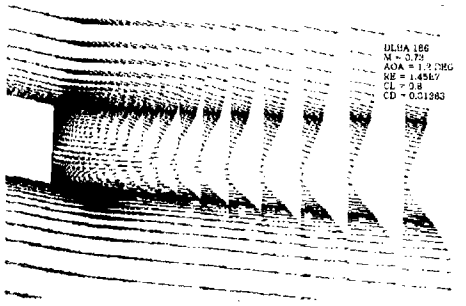

Fig.7a Velocity Field behind the Trailing Edge of DLBA 186

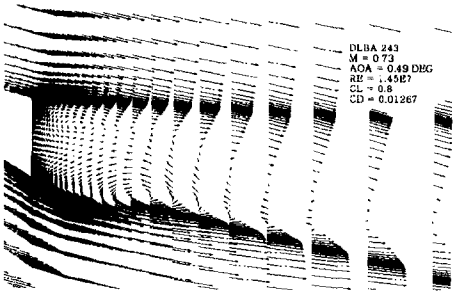

Fig.7b Velocity Field behind the Trailing Edge of DLBA 243

4. CONCLUSION

The calculated results represented here are subject to uncertainties that result from numerical, boundary condition, and turbulence model assumptions which are difficult to isolate. Uncertainties associated with boundary conditions and mesh densities are estimated to contribute less than 0.3% to lift and 6% to drag based on the grid studies reported above. Measured and calculated flow structures, sensibly describe the shock, boundary layer and recirculating flow, and, in combination with the cited experiments, provide insights that lead to the following statements.

Comparison of calculations of DLBA 243 DTE and DLBA 186 seed airfoils at the same Reynolds and Mach number, shows the following:

- Reduction in drag is due to a decrease in the shock-induced drag, resulting from a delayed and weakened shock, which is greater than the increase in base drag.
- At the same lift coefficient, drag creep can be reduced at transonic cruise speeds on supercritical airfoils by DTE modification. There is an improvement in lift-to-drag ratio.
- Pressure difference between pressure and suction side of DTE airfoils is more constant from the suction-side shock aft to the trailing edge than the seed airfoil.
- DTE modification also increases the size of the recirculation region downstream of a blunt trailing edge.

후 기

본 연구는 '95년도 강원대학교 학술진흥재단의 해외연구지원에 의하여 이루어졌으며, 이에 감사드립니다.

REFERENCES

1. Whitcomb, R.T., "Review of NASA Supercritical Airfoils", Proceedings of the Ninth International Congress of the International Council of the Aeronautical Sciences (ICAS), 1974.

2. Bauer, F., Garabedian, P., Korn, D., and Jameson. A., Supercritical Wing Sections II, Lecture Notes in Economics and Mathematical Systems, Vol. 108, Springer-Verlag, New York, 1975.

3. Harris, C.D., "Wind Tunnel Investigation of Effects of Trailing Edge Geometry on a NASA Supercritical Airfoil Section," NASA TM-X-2336, 1971.

4. Henne, P.A., and Gregg, R.D., "New Airfoil Design Concept," Journal of Aircraft, May, 1991, pp. 300-311.

5. Lotz, R. D., Thompson, B.E., Davoudzadeh, F., and Konings, C. "Grid Dependence and

Numerical Uncertainty Analysis of a Transonic Airfoil Calculation", RWJ-10-94, joint JSME/ASME Fluids Engineering Conference, August 13-18, 1995.

6. Henne, P. A., "Innovation with Computational Aerodynamics : The Divergent Trailing Edge Airfoil", Applied Computational Aerodynamics, edited by P.A. Henne, AIAA Inc., Washington, D.C., 1990.

7. Thompson, B.E., and Whitelaw, J.H., "Trailing Edge Region of Airfoils," Journal of Aircraft, March,1989,pp.225- 234.

8. Briley, W.R. and McDonald, H. "Solution of the Multidimensional Compressible Navier Stokes Equations by a Generalized Implicit Method," Journal of Computational Physics, vol. 24, 1977, pp. 372-397.

9. Liu, N. S., Davoudzadeh, F., Briley, W.R., and Shamroth, S.J. "Navier-Stokes Simulation of Transonic Blade-Vortex Interactions," Journal of Fluids Engineering, vol. 112, Dec. 1990, pp. 501-509. 10. Kline, S.J., Cantwell, B.J., and Lilley, G.M. editors, "1980-81 AFOSR HTTM Stanford Conference on Complex Turbulent Flows: Comparison of Computation and Experiments." Thermosciences Division, Mechanical Engineering Dept., Stanford University, Stanford, California, Sept. 3-6, 1980.

11. Locke, R.C. and Williams, B.R., "Viscous Inviscid Interactions in External Aerodynamics", Progress of Aerospace Science, Vol. 24, 1987, pp. 51-76.

12. Roscoe, D.V., Gibeling, H.J., McDonald, H., and Shamroth, S.J., "Development of a Navier-Stokes Analysis to Investigate the Mechanism of Shock-Wave-Boundary- Layer Interactions," Numerical and Physical Aspects of Aerodynamic Flows III (ed. T. Cebeci), Springer-Verlag, New York, 1985.